Available online at www.sciencedirect.com
ScienceDirect
Journal of Photochemistry and Photobiology A: Chemistry 188 (2007) 392–398
Journal of Photochemistry and Photobiology A:Chemistry
www.elsevier.com/locate/jphotochem

Photo-Fenton defluoridation of pentafluorobenzoic acid with UV-C light

L. Ravichandran, K. Selvam, M. Swaminathan *

Department of Chemistry, Annamalai University, Annamalainagar 608 002, Tamilnadu, India

Received 15 September 2006; received in revised form 26 December 2006; accepted 30 December 2006
Available online 4 January 2007

Abstract

Photocleavage of C–F bond in pentafluorobenzoic acid (PFBA) has been carried out using ferrous sulphate/ferrioxalate with H_2O_2 and UV light. The defluoridation was monitored by the ionometer with fluoride ion selective electrode. The rate of photodefluoridation is higher with the light of 254 nm than with 365 nm. Ferrioxalate process is more efficient than ferrous photo-Fenton process. The effects of various experimental parameters such as pH, initial H_2O_2, Fe^{2+}, Fe^{3+}, initial PFBA concentration and airflow rate have been investigated. The addition of TiO_2-P25 to these processes strongly influenced the defluoridation of PFBA. The GC–MS analysis of PFBA solution after irradiation with photo-Fenton processes reveals the formation of pentafluorobenzene, pentafluorophenol and tetrafluoroquinone as intermediates. The optimum operating conditions for efficient defluoridation are reported.

Keywords: Pentafluorobenzoic acid; Photo-Fenton defluoridation; Ferrous ion; Ferrioxalate/H_2O_2; UV-C light

1. Introduction

Organic fluorochemical compounds are widely used in a variety of industrial and commercial application as polymer additives, lubricants, fire retardants and suppressants, pesticides and surfactants [1] and are detected in environmental waters [2], wild animals [3] and human serum [4]. Among these, the perfluorinated acids are quite stable and they have no known natural decomposition [5]. The defluoridation of these acids results in the formation of fluoride ions, which can easily combine with Ca^{2+} to form environmentally harmless CaF_2. In addition, CaF_2 is a raw material for the production of hydrofluoric acid, which is a starting material for many fluorinated compounds. Hori et al. reported the photocatalytic cleavage of the strong C–F bond (485.3 kJ mol^{-1}) in pentafluoropropionic acid with a water-soluble heteropoly acid [$H_3PW_{12}O_{40}$] photocatalyst [6].

A review on microbial cleavage of C–F bond had been published recently [7]. In recent years, advanced oxidation processes (AOPs) have been widely used for the destruction and mineralization of non-biodegradable organic pollutants in wastewater. The AOPs, almost rely on the generation of very reactive free radicals, such as hydroxy radical ($^{\bullet}OH$). These radicals react rapidly and mineralize most of the organic compounds to CO_2 and H_2O. Among the AOPs photo-Fenton process was reported to be more economical [8]. In the photo-Fenton processes use of ferrioxalate is found to be more advantageous than the ferrous and other ferric salts. The usefulness and applicability of UV/vis/ferrioxalate/H_2O_2 process as compared to the UV/H_2O_2 and UV/vis/Fe(II)/H_2O_2 processes had been well-demonstrated [9]. Pentafluorobenzoic acid (PFBA) is used as a fluoroaromatic intermediate in manufacture of some drugs and as a catalyst for polymerization process. This is the continuation of work on degradation of dyes and fluoro compounds by various advanced oxidation processes [10–15].

In the present work we have investigated the photodefluoridation of pentafluorobenzoic acid using ferrous sulphate/ferrioxalate with H_2O_2 and UV-C-light (254 nm) and analyzed the effects of various experimental parameters such as pH, initial H_2O_2, Fe^{2+}, Fe^{3+}, initial PFBA concentration and airflow rate on these processes.

2. Experimental

2.1. Materials

Pentafluorobenzoic acid (99% purity) was obtained from Aldrich Chemical Co. and was used without further purifica-

* Corresponding author. Tel.: +91 4144 220572; fax: +91 4144 220572.
E-mail address: chemsam@yahoo.com (M. Swaminathan).

1010-6030/$ – see front matter © 2007 Elsevier B.V. All rights reserved.
doi:10.1016/j.jphotochem.2006.12.041

tion. A gift sample of TiO_2-P25 was obtained from Degussa (Germany). It has the particle size of 30 nm and BET specific surface area of 55 m^2/g. Potassium ferrioxalate $K_3[Fe(C_2O_4)_3]$ was prepared and purified by recrystallization using water [16]. Double distilled water was used to prepare experimental solutions. The pH of the solutions was adjusted using H_2SO_4 or NaOH.

2.2. Irradiation experiments

For the photolysis experiment, a desired molar ratio of PFBA/$Fe^{2+/3+}$/H_2O_2 solutions were freshly prepared from stock solutions of $FeSO_4 \cdot 7H_2O$, $K_2[Fe(C_2O_4)_3]$ and H_2O_2. All photochemical reactions were carried out under identical conditions using Heber photoreactor model HML-MP HIPR-LP 6/8/116 whose schematic diagram is reported in our previous paper [15]. This model consisted of a double walled immersion well made of a quartz reactor of 175 cm^3 capacity. A small diameter inlet tube extended down the annular space to ensure flow of the coolant from bottom of well upward to outlet. In the center of cylindrical reactor, the lamp used for light source was placed inside the quartz tube. For the experiments, lamps with different wavelength emission were used. One was 16 W low-pressure mercury with emission mainly on the mercury resonance line at 253.7 nm. The other lamp was 8 W medium pressure mercury lamp with broadband emission predominantly emitting at 365 nm. For both the lamps photon flux of the light source was determined by ferrioxalate actinometry and the values are: 16 W low-pressure Hg lamp $I_{254\,nm} = 2.54 \times 10^{-5}$ Einstein L^{-1} s^{-1}, 8 W medium pressure Hg lamp $I_{365\,nm} = 2.08 \times 10^{-6}$ Einstein L^{-1} s^{-1}. The reaction vessel had an arm at the top for gas purging and the air was passed into the solution by bubbling. The temperature of the experimental solution was maintained at 25 ± 1 °C by circulating water during the experiments.

2.3. Defluoridation analysis

Fluoride ion concentration was determined using Orion expandable ion analyzer model (EA940). The analysis was done using fluoride ion selective electrode in conjugation with Ag/AgCl reference electrode. The instrument was calibrated using standard sodium fluoride solutions of various concentrations between 10 and 250 ppm of fluoride ion. The sample from photochemical reactor was taken into 50 mL of polyethylene beaker at a regular interval of 30 min. Five millilitres of water and 20 mL of ionic strength adjustable buffer (TISAB) were added to the solution. This solution was stirred for 5 min and fluoride ion concentration was measured. The pH of the solutions was measured using Metrohm 744 pH meter.

2.4. GC–MS analysis

For identification of intermediate products of PFBA photocatalytic defluoridation, the samples taken after 30, 60 and 90 min were analyzed. NaOH solution was used to quench the oxidation by raising the pH to10. At this pH Fe^{3+} is converted into a hydroxo complex and this prevents generation of hydroxyl radical. The sample for analysis was prepared by the following method. The experimental solutions obtained after irradiation was extracted five times with HPLC grade dichloromethane. The extract was dried over anhydrous sodium sulphate to remove the water present in the solution. The solvent was removed by evaporation under reduced pressure. The final residual mass was taken for GC–MS analysis.

The GC (Perkin-Elmer Auto System) is equipped with an MSHP 5 capillary column (30 μm × 250 μm) and 1 μm film thickness (Perkin-Elmer elite series) and interfaced directly to the MS (Perkin-Elmer turbo mass spectrophotometer). The GC column was operated at a temperature of 50 °C for 2 min then increased to 280 °C at the rate of 10 °C min^{-1}. The other experimental conditions are: EI impact ionization 70 eV, helium as carrier gas, injection temperature 260 °C, source temperature 180 °C.

3. Results and discussion

3.1. Primary analysis

Initially, the photodefluoridation of pentafluorobenzoic acid by ferrous sulphate and ferrioxalate systems including Fe^{2+}/UV, Fe^{3+}/UV, Fe^{2+}/H_2O_2/UV, Fe^{3+}/H_2O_2/UV, H_2O_2/UV and UV only have been carried out for the comparison of the efficiencies and the results are presented in Table 1. From the results, it is clear that the photodefluoridation of PFBA to fluoride ions by direct photolysis and irradiation in the presence of ferrous ion alone was observed at a much slower rate. After 30 min of irradiation time 28.6 mg/L of fluoride ion was released by ferrioxalate/UV process. The photodefluoridation of PFBA on

Table 1
Primary analysis of photodefluoridation of PFBA

Process	Condition[a]	Reaction time (min)	$[F^-]$ (mg/L)
(1) PFBA/UV		150	11.2
(2) PFBA/ferrous/UV	Ferrous (0.1 mmol)	150	18.7
(3) PFBA/ferric/UV	Ferric (0.1 mmol)	30	28.6
(4) PFBA/H_2O_2/UV	H_2O_2 (10 mmol)	30	32.1
(5) PFBA/ferrous/H_2O_2/dark	Ferrous (0.1 mmol); H_2O_2 (10 mmol)	30	43.2
(6) PFBA/ferric/H_2O_2/dark	Ferric (0.1 mmol); H_2O_2 (10 mmol)	30	17.0
(7) PFBA/ferrous/H_2O_2/UV	Ferrous (0.1 mmol); H_2O_2 (10 mmol)	30	61.0
(8) PFBA/ferric/H_2O_2/UV	Ferric (0.1 mmol); H_2O_2 (10 mmol)	30	82.4

[a] PFBA = 400 ppm; pH 3 ± 0.1 for all reactions.

irradiation in the presence of ferrioxalate is due to the formation of hydroxyl radical during its photolysis (Eqs. (1)–(6)).

$$Fe(III)(C_2O_4)_3^{3-} + h\nu \rightarrow Fe^{2+} + 2C_2O_4^{2-} + C_2O_4^{\bullet -} \quad (1)$$

$$C_2O_4^{\bullet -} \rightarrow CO_2^{\bullet -} + CO_2 \quad (2)$$

$$CO_2^{\bullet -} + O_2 \rightarrow CO_2 + O_2^{\bullet -} \quad (3)$$

$$O_2^{\bullet -} + H^+ \rightarrow HO_2^{\bullet} \quad (4)$$

$$HO_2^{\bullet} + HO_2^{\bullet} \rightarrow H_2O_2 + O_2 \quad (5)$$

$$H_2O_2 + Fe^{2+} \rightarrow Fe^{3+} + {}^{\bullet}OH + OH^- \quad (6)$$

Zuo and Hoigne [17] reported the formation of H_2O_2 in ferrioxalate photolysis and it is related to pH, irradiation intensity and the concentration of ferrioxalate. For Fe^{2+}/H_2O_2 and Fe^{3+}/H_2O_2 the defluoridation of PFBA to fluoride ions of 43.29 and 17.69 mg/L were observed in dark for 30 min. A higher defluoridation was obtained in ferrous/H_2O_2 due to the production of hydroxyl radical in the process. Though the ferric ion catalyzes the decomposition of H_2O_2 in dark [18], its efficiency is very low when compared to ferrous ion. Hence, the defluoridation in Fe^{3+}/H_2O_2/dark process was 17.6 mg/L whereas in Fe^{2+}/H_2O_2/dark defluoridation was 43.2 mg/L in 30 min. This is because of the low reactivity of ferric ion towards hydrogen peroxide in dark. This iron complex generates Fe(II) only on irradiation and hence the efficiency is very much increased for Fe^{3+}/H_2O_2 when irradiated. Irradiation with Fe^{3+}/H_2O_2 causes 82.4 mg/L of fluoride ion removal.

In Fe^{2+}/H_2O_2/UV process the defluoridation is due to generation of hydroxyl radical by: (i) Fenton reaction (Eq. (6)), (ii) direct photolysis of H_2O_2 (Eq. (7)) and (iii) photo reduction of Fe^{3+} formed during the irradiation (Eq. (8)).

$$H_2O_2 + h\nu \rightarrow {}^{\bullet}OH + OH^- \quad (7)$$

$$Fe^{3+} + H_2O + h\nu \rightarrow {}^{\bullet}OH + Fe^{2+} + H^+ \quad (8)$$

However, in Fe^{2+}/H_2O_2/UV process reactions (7) and (8) contribute less to defluoridation of PFBA (Table 1). In Fe^{3+}/H_2O_2/UV process the defluoridation of PFBA is due to the fast generation of Fe^{2+} ion by photolysis of ferrioxalate (Eq. (1)). A greater enhancement of defluoridation rate was observed in Fe^{3+}/H_2O_2/UV over Fe^{3+}/H_2O_2/dark. This enhancement is due to light absorption of ferrioxalate strongly at longer wavelength generating Fe^{2+} ion with high quantum yield. The reported quantum yield of Fe(II) generation is nearly constant (1.0–1.2) for the irradiation with the light in the range of 250–450 nm [19].

The relative efficiencies of the above processes are in the following order: PFBA/Fe^{3+}/dark < PFBA/Fe^{3+}/UV < PFBA/H_2O_2/UV < PFBA/Fe^{2+}/H_2O_2/dark < PFBA/Fe^{2+}/H_2O_2/UV < PFBA/Fe^{3+}/H_2O_2/UV.

Between two photo-Fenton processes, the Fe^{3+}/H_2O_2/UV process is found to be more efficient than Fe^{2+}/H_2O_2/UV process. This is because of the high molar absorption coefficient of ferrioxalate for the wavelengths above 200 nm [9]. The photodefluoridation of pentafluorobenzoic acid by these photo-Fenton processes was studied as a function of pH, initial H_2O_2, Fe^{2+}, Fe^{3+}, initial PFBA concentration and airflow rate.

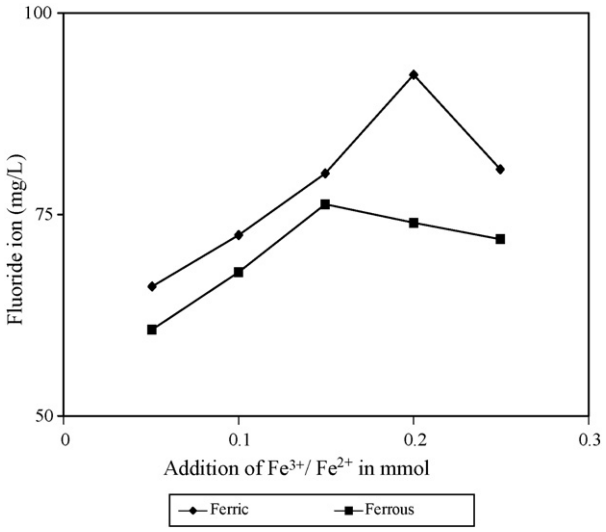

Fig. 1. Amount of ferrous and ferrioxalate dosage on defluoridation of PFBA. [PFBA] = 400 ppm; H_2O_2 = 10 mmol, pH = 3; irradiation time = 20 min, airflow rate = 8.1 mL s^{-1}; $I_{254\,nm} = 2.54 \times 10^{-5}$ Einstein L^{-1} s^{-1}.

3.2. Optimization of reaction conditions

3.2.1. Amount of Fe^{2+} and Fe^{3+} dosage

The photodefluoridation of pentafluorobenzoic acid is represented as a function of initial Fe^{2+} and Fe^{3+} dosages. The results are shown in Fig. 1. Increase of Fe^{2+} dosage from 0.05 to 0.15 mmol increases the defluoridation from 60.6 to 76.3 mg/L in 20 min. Further increase has no significant effect. The increase in the removal rate is due to increase in the hydroxyl radical production by ferrous ion. In Fe^{3+} process increase of initial Fe^{3+} concentration from 0.1 to 0.2 mmol increases the defluoridation from 72.4 to 92.43 mg/L in 20 min. Further increase from 0.2 to 0.25 mmol decreases the removal rate. The generation of Fe^{2+} is likely to be the main step of photodefluoridation in ferrioxalate system.

Since the light absorption fraction of Fe^{3+}, particularly at longer wavelength region, is greater than Fe^{2+}, the increase of ferrioxalate concentration increases photon absorption producing more Fe^{2+} ion. The higher quantum yield of formation of Fe(II) from ferrioxalate above one in the wavelength region 250–400 nm also confirms this.

This results in the increase of defluoridation rate. But when the ferrioxalate concentration is above 0.2 mmol the light penetration through the irradiated solution decreases and the ferrioxalate at higher concentrations produces less reactive hydroperoxy radicals [20]. 0.1 mmol of Fe^{2+} and 0.15 mmol Fe^{3+} are optimum dosages for Fe^{2+}/H_2O_2/UV and Fe^{3+}/H_2O_2/UV processes, respectively.

$$Fe^{3+} + H_2O_2 \rightarrow Fe^{2+} + HO_2^{\bullet} + H^+ \quad (11)$$

3.2.2. Amount of added H_2O_2

The initial concentration of H_2O_2 plays a very important role in the oxidation of organic compounds in photo-Fenton processes. Fig. 2 shows the effect of addition of H_2O_2 on the ferrous and ferric photo-Fenton defluoridation of PFBA to fluoride ions.

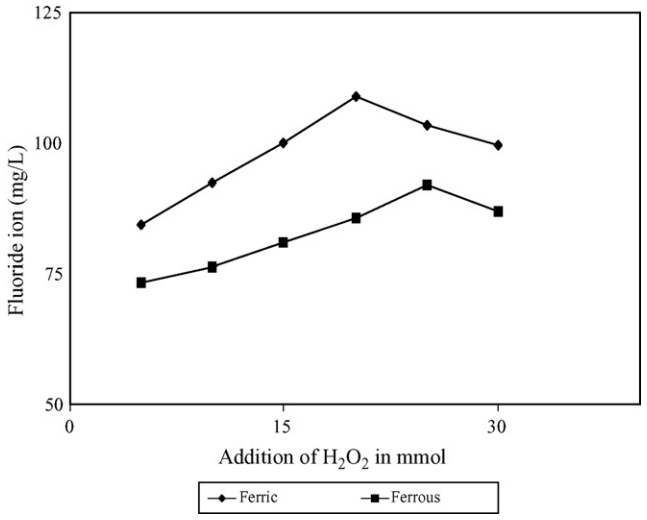

Fig. 2. The effect of addition of H_2O_2 on defluoridation of PFBA. [PFBA] = 400 ppm; Fe^{3+} = 0.2 mmol; Fe^{2+} = 0.15 mmol, pH = 3; irradiation time = 20 min; airflow rate = 8.1 mL s^{-1}; $I_{254\,nm} = 2.54 \times 10^{-5}$ Einstein L^{-1} s^{-1}.

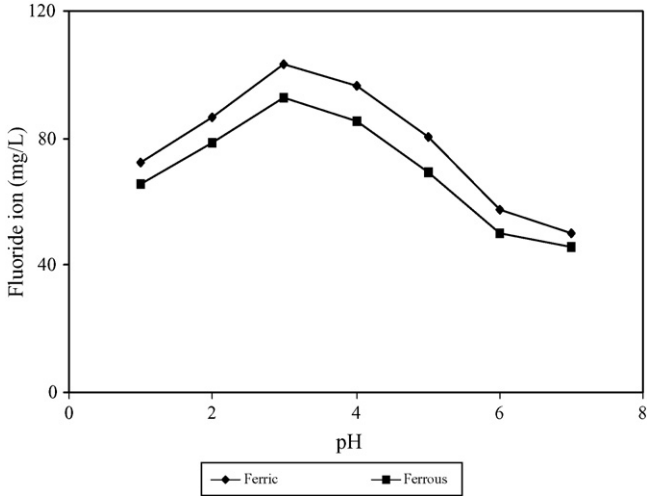

Fig. 3. The effect of pH on defluoridation of PFBA. [PFBA] = 400 ppm; Fe^{3+} = 0.2 mmol; Fe^{2+} = 0.15 mmol; H_2O_2 = 20 mmol; irradiation time = 20 min; airflow rate = 8.1 mL s^{-1}; $I_{254\,nm} = 2.54 \times 10^{-5}$ Einstein L^{-1} s^{-1}.

Addition of H_2O_2 increases the fluoride formation rate in both processes up to a certain concentration. In ferrous photo-Fenton process for 20 min irradiation, addition of 10–30 mM of H_2O_2 increases the fluoride formation rate. Further addition of H_2O_2 above 30 mmol decreases the formation rate. Hence, 30 mmol of H_2O_2 is found to be optimum for ferrous process. For ferric process addition of H_2O_2 up to 20 mmol increases the defluoridation from 84.5 to 108.8 mg/L after 20 min irradiation. Further increase of H_2O_2 dosage decreases the defluoridation rate. The optimum concentration of H_2O_2 for ferric process is 20 mmol. The enhancement of defluoridation is due to the increased production of hydroxyl radicals by these processes.

$$H_2O_2 + e_{CB}{}^- \rightarrow {}^\bullet OH + OH^- \quad (12)$$

$$H_2O_2 + O_2{}^{\bullet -} \rightarrow {}^\bullet OH + H^+ + O_2 \quad (13)$$

At excess dosage the defluoridation rate decreases due to its hydroxyl radical and hole scavenging effects (Eq. (14)–(16)).

$$H_2O_2 + {}^\bullet OH \rightarrow HO_2{}^\bullet + H_2O \quad (14)$$

$$HO_2{}^\bullet + {}^\bullet OH \rightarrow H_2O + O_2 \quad (15)$$

$$H_2O_2 + h^+ \rightarrow HO_2{}^\bullet + H^+ \quad (16)$$

3.2.3. Effect of pH

pH is an important parameter for photo-Fenton processes. The pH of the solution controls the production rate of hydroxyl radical, concentration and the nature of iron species in solution. The effects of pH on defluoridation rate of PFBA are shown in Fig. 3. The results indicate that both processes are efficient at pH 3. Increase of pH from 1 to 3 increases the defluoridation. Above pH 3 the defluoridation decreases in both processes. It was reported that the optimum pH in photo-Fenton processes is pH 3 [11]. In photo-Fenton processes the photodefluoridation increases from 1 to 3 and decreases from pH 3 to 7. In these processes the decrease in defluoridation at pH above 3 is due to the coagulation of hydroxo complex of Fe^{3+} formed during the reaction [21].

3.3. Factors influencing photo-Fenton defluoridation of PFBA

The photodefluoridation of PFBA was studied as a function of addition of TiO_2-P25 on ferrous and ferric photo-Fenton processes with 254 and 365 nm light and the results are given in Table 2. The results clearly indicate that TiO_2-P25 exhibits sustainable catalytic activity in both ferrous and ferric processes. Addition of 175 mg of TiO_2-P25 increases the defluoridation from 103.4 to 128.5 mg/L in ferric photo-Fenton process and from 92.9 to 102.3 mg/L in ferrous photo-Fenton process at the time of 20 min. In both processes enhancement of defluoridation is due to: (i) increase of hydroxyl radical concentration; (ii) increase in the absorption of light. The effect of initial PFBA concentrations from 200 mg to 600 mg/L on the defluoridation rate at constant pH and catalyst loading is shown in Fig. 4. From the figure it is clear that increase of PFBA initial concentration decreases its defluoridation rate. The increase of the photodefluoridation as a function of airflow rate reveals the enhancement of photodefluoridation by oxygen (Fig. 5).

Table 2
Effect of addition of TiO_2 on PFBA

TiO_2	Ferric process [F^-] (mg/L)		Ferrous process [F^-] (mg/L)	
	254 nm	365 nm	254 nm	365 nm
Without	103.4	15.6	92.9	13.2
With TiO_2	128.5	46.8	102.3	35.6

Ferrous process: [PFBA] = 400 ppm; Fe^{3+} = 0.2 mmol; H_2O_2 = 25 mmol; irradiation time = 20 min; airflow rate = 8.1 mL s^{-1}; $I_{254\,nm} = 2.54 \times 10^{-5}$ Einstein L^{-1} s^{-1}.
Ferrioxalate process: [PFBA] = 400 ppm; Fe^{2+} = 0.15 mmol; H_2O_2 = 20 mmol; irradiation time = 20 min; airflow rate = 8.1 mL s^{-1}; $I_{254\,nm} = 2.54 \times 10^{-5}$ Einstein L^{-1} s^{-1}.

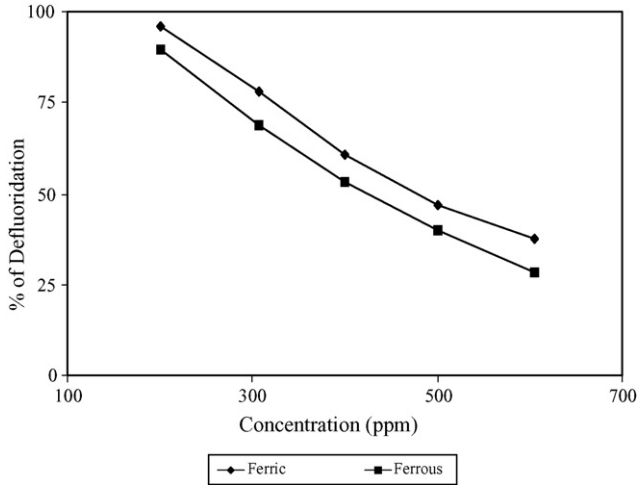

Fig. 4. The effect of various initial PFBA concentration on defluoridation. [PFBA] = 400 ppm; Fe^{3+} = 0.2 mmol; Fe^{2+} = 0.15 mmol; H_2O_2 = 20 mmol; irradiation time = 20 min; airflow rate = 8.1 mL s^{-1}; $I_{254\,nm}$ = 2.54 × 10^{-5} Einstein L^{-1} s^{-1}.

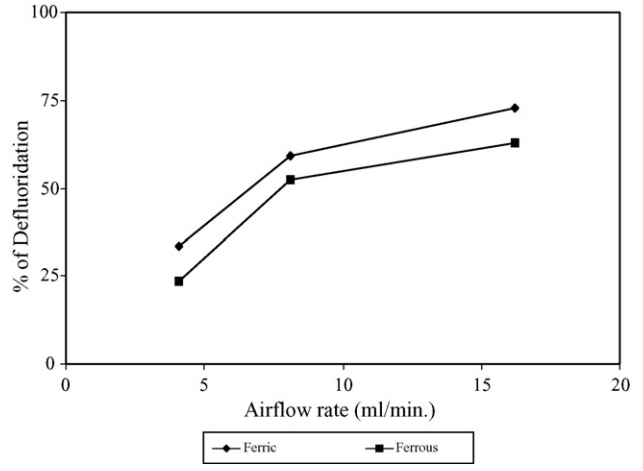

Fig. 5. The effect of airflow rate on defluoridation of PFBA. [PFBA] = 400 ppm; Fe^{3+} = 0.2 mmol; Fe^{2+} = 0.15 mmol; H_2O_2 = 20 mmol; irradiation time = 20 min; $I_{254\,nm}$ = 2.54 × 10^{-5} Einstein L^{-1} s^{-1}.

The effect of passing air, oxygen and nitrogen on photodefluoridation of PFBA was investigated and results are presented in Table 3. It has been observed that dissolved oxygen has a very weak effect. When air was replaced by oxygen, the defluoridation rate increased sharply. In contrary, the replacement of oxygen by nitrogen decreases PFBA defluoridation rate by 20% at the time 20 min. This indicates that without passing O_2 or air to reaction mixture PFBA cannot undergo effective defluoridation.

Table 3
Effect of oxygen on photodefluoridation of PFBA

Gas	Percentage of defluoridation	
	Ferric process	Ferrous process
Air	57.46	51.61
O_2	86.78	70.43
N_2	31.09	25.67

Ferrous process: [PFBA] = 400 ppm; Fe^{3+} = 0.2 mmol; H_2O_2 = 25 mmol; irradiation time = 20 min; airflow rate = 8.1 mL s^{-1}; $I_{254\,nm}$ = 2.54 × 10^{-5} Einstein L^{-1} s^{-1}.
Ferrioxalate process: [PFBA] = 400 ppm; Fe^{2+} = 0.15 mmol; H_2O_2 = 20 mmol; irradiation time = 20 min; airflow rate = 8.1 mL s^{-1}; $I_{254\,nm}$ = 2.54 × 10^{-5} Einstein L^{-1} s^{-1}.

Table 4
Comparison of efficiencies in photo-Fenton and UV/TiO_2-processes

Process	[F^-] (mg/L)	
	254 nm	365 nm
UV/TiO_2	80.2	24.2
Photo-Fenton	103.4	15.6

[PFBA] = 400 ppm; Fe^{2+} = 0.15 mmol; H_2O_2 = 20 mmol; irradiation time = 20 min; airflow rate = 8.1 mL s^{-1}; $I_{254\,nm}$ = 2.54 × 10^{-5} Einstein L^{-1} s^{-1}, TiO_2-P25 = 175 mg; $I_{365\,nm}$ = 2.08 × 10^{-6} Einstein L^{-1} s^{-1}.

Investigation of photodefluoridation using 254 nm mercury lamp [I = 2.54 × 10^{-5} Einstein L^{-1} s^{-1}] and 365 nm [I = 2.381 × 10^{-6} Einstein L^{-1} s^{-1}] separately under identical conditions reveals that high-energy radiation is more effective in bringing out photodefluoridation of PFBA. This is because the 254 nm light having high intensity and absorbance increases the direct formation of OH radical and the quantum yield of photo reduction of Fe^{3+} to Fe^{2+}. A significant increase in the quantum yield of reduction of Fe^{3+} to Fe^{2+} from 0.017 to 0.140 was reported when the irradiation wavelength was decreased from 360 to 313 nm [22].

Since Fe^{3+}/H_2O_2/UV is found to be more efficient, the defluoridation efficiency of this process is compared with the defluoridation efficiency of reported UV/TiO_2 process [14] in Table 4. The results indicate that photo-Fenton process is more efficient than UV/TiO_2 at 254 nm light whereas at 365 nm light UV/TiO_2 is slightly more efficient. The higher efficiency of UV/TiO_2 at 365 nm is due to the higher absorption of 365 nm by TiO_2.

From Table 4, one can see that PFBA can be effectively degraded in Photo-Fenton process on irradiation with UV-C light. The C–F bond is one of the strongest covalent bonds known. The fluorine atom is larger than the hydrogen atom, so it shields the carbon from attack more effectively than hydrogen atoms. In fluoro carbons C–C bond energy is 334.7 kJ mol^{-1}, whereas C–F bond energy is 485.3 kJ mol^{-1} [23]. Hence, more energy is required to break C–F bond than C–C bond. The release of fluoride ion and carbon dioxide from PFBA on irradiation with 254 nm light indicates that PFBA can be effectively mineralized into CO_2 and fluoride ions.

Addition of ethanol [0.1 M] decreases the photodefluoridation efficiency of both ferrous and ferric processes. It was observed that small amount of ethanol inhibited the defluoridation of PFBA. This reveals that ethanol quenches the OH radical formation. The rate constant of reaction between hydroxyl radical and ethanol was reported to be 1.9 × 10^{-1} M^{-1} s^{-1} [24].

3.4. Proposed defluoridation pathway

Irradiation of air equilibrated aqueous solution of pentafluorobenzoic acid with UV 254 nm light using ferrous

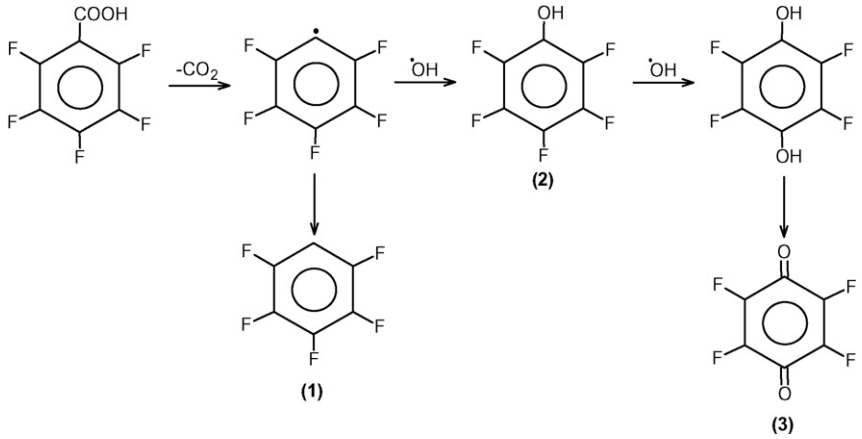

Scheme 1.

sulphate/ferrioxalate and H_2O_2 leads to conversion of fluorinated derivatives into detectable intermediate aromatic products and eventually to the evolution of stoichiometry quantities of fluoride and carbon dioxide.

An attempt was made to identify the intermediate products formed in the photo-Fenton defluoridation of the pentafluorobenzoic acid through GC–MS analysis of the solution obtained after 20 and 40 min irradiation. The total ion chromatogram is given in Fig. 6. We get three predominant peaks for retention times of 2.18, 19.4 and 20.2 min. These three products were identified as pentafluorobenzene (**1**), pentafluorophenol (**2**) and tetrafluoroquinone (**3**) based on their molecular ion and mass spectrometric fragmentation peaks and they are given below.

Compound	Mass spectrum (*m*/*z*)
1	168, 149, 137, 118, 99, 84, 75, 61, 51, 47, 31
2	181, 163, 149, 135, 121, 112, 104, 92, 77, 56, 41, 29
3	184, 168, 156, 142, 128, 112, 100, 84, 70, 58, 44, 41

From Scheme 1, first band cleaved in the one electron oxidized PFBA is the C–C bond between C_6F_5 and COOH. This cleavage produces $C_6F_5^{\bullet}$ and CO_2.

Pentafluorobenzene (**1**) is formed from $C_6F_5^{\bullet}$. This photokolbe mechanism was proposed for a similar cleavage reported in pentafluoropropionic acid [7] and trifluoroacetic acid [25]. The attack of OH radical on $C_6F_5^{\bullet}$ may produce pentafluorophenol (**2**), which produce tetrafluoroquinone (**3**). In general, the attack of PFBA by OH radical replaces fluorine atoms producing more hydroxyl functional groups and the intermediates are ultimately mineralized to carbon dioxide and fluoride ions. A similar kind of mineralization has been reported for pentafluorophenol [26].

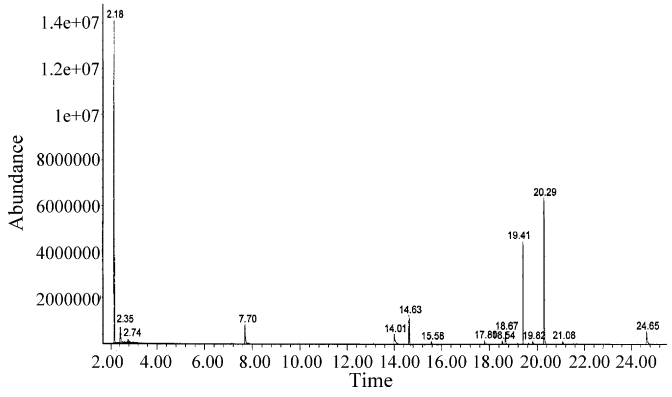

Fig. 6. The total ion chromatogram of PFBA.

4. Conclusions

Pentafluorobenzoic acid is effectively deflouridated by the ferrous and ferric photo-Fenton processes with UV 254 nm light. The ferric process is the most efficient among all the processes. The defluoridation efficiency is maximum at 0.15 mmol of Fe^{2+} and 25 mmol of H_2O_2 for ferrous photo-Fenton and 0.2 mmol of Fe^{3+} and 20 mmol of H_2O_2 for ferric photo-Fenton process. Both processes are efficient at pH 3 and decrease at both sides. The rate of photodefluoridation is higher with the light of 254 nm than with 365 nm. Addition of TiO_2-P25 increases the efficiency of ferric photo-Fenton process more than ferrous photo-Fenton process. The deflouridation rate decreases with the increase in initial PFBA concentrations. It is found that both the ferrous and ferric processes are viable and more efficient than UV/TiO_2 process for the treatment of wastewater containing PFBA within a short time.

Acknowledgement

The authors thank the Research and Development Section of Sriram Fibers Limited, Chennai, for recording GC–MS spectra.

References

[1] B.D. Key, R.D. Howell, C.S. Criddle, Environ. Sci. Technol. 31 (1997) 2445–2454.
[2] E. Sinclair, S. Taniyasu, N. Yamashita, K. Kannan, Organohalogen Compd. 66 (2004) 4069–4073.
[3] K. Kannan, L. Tao, E. Sinclair, S.D. Pastva, D.J. Jude, J.P. Giesy, Arch. Environ. Contam. Toxicol. 48 (2005) 559–566.
[4] K.S. Guruge, S. Taniyasu, N. Yamashita, S. Wijeratna, K.M. Mohotti, H.R. Senevriatne, K. Kannan, N. Yamashita, S. Miyazaki, J. Environ. Monit. 7 (2005) 371–377.
[5] R. Renner, Environ. Sci. Technol. 35 (2001) 154A–160A.
[6] H. Hori, Y. Takano, K. Koike, S. Kutsuna, H. Einaga, T. Ibusuki, Appl. Catal. B: Environ. 46 (2003) 333.

[7] R. Natarajan, R. Azerad, B. Badet, E. Copin, J. Fluorine Chem. (2005) 424–435.
[8] M. Muruganandam, K. Selvam, M. Swaminathan, J. Hazard. Mater., doi:10.1016/j.jhazmat.2006.10.035.
[9] A. Safarzadeh-Amiri, J.R. Bolton, S.R. Cater, Water Res. 31 (4) (1997) 787–798.
[10] K. Selvam, M. Muruganandham, M. Swaminathan, Sol. Energy Mater. Sol. Cells 89 (2005) 61–74.
[11] M. Muruganandham, M. Swaminathan, Sol. Energy Mater. Sol. Cells 81 (2004) 439–457.
[12] M. Muruganandham, M. Swaminathan, Dyes Pigments 62 (2004) 271–277.
[13] M. Muruganandham, M. Swaminathan, Dyes Pigments 63 (2004) 315–321.
[14] M. Muruganandham, M. Swaminathan, J. Mol. Catal. 246 (2005) 154–161.
[15] L. Ravichandran, K. Selvam, M. Muruganandham, M. Swaminathan, J. Fluorine Chem. 127 (2006) 1204–1210.
[16] C.G. Hatchard, C.A. Parker, Proc. R. Soc. London A 235 (1956) 518–536.
[17] Y. Zuo, J. Hoigne, Environ. Sci. Technol. 26 (1992) 1014–1022.
[18] C. Walling, Acc. Chem. Res. 8 (1975) 125–131.
[19] V. Balzani, V. Carassiti, Photochemistry of Coordination Compounds, Academic Press, London, 1970, p. 145.
[20] C.Y. Kwan, W. Chu, Water Res. 37 (2003) 4405–4412.
[21] E.G. Solozhenko, N.M. Soboleva, V.V. Goncharuk, Water Res. 29 (1995) 2206–2210.
[22] B.C. Faust, J. Hoigne, Atmos. Environ. 24A (1990) 78–89.
[23] T. Hiyama, Organofluorine Compounds: Chemistry and Applications, Springer Verlag, Berlin, 2000, pp. 1–23.
[24] Y. Lee, J. Jeong, C. Lee, S. Kim, J. Yoon, Chemosphere 51 (2003) 901–912.
[25] H. Hori, Y. Takano, K. Koike, K. Takeuchi, H. Einaga, Environ. Sci. Technol. 37 (2003) 418–422.
[26] C. Minero, E. Pelizzetti, Langmuir 10 (1994) 692–698.